Diode laser spectroscopic measurements and theoretical calculations of line parameters of nitrogen broadened water vapor overtone transitions in the 818-834 nm wavelength region

Amitava Bandyopadhyay[1], Biswajit Ray[1], Pradip N. Ghosh[1*], Danielle L. Niles[2] and Robert R. Gamache[2#]

[1]Department of Physics, University of Calcutta

92, A. P. C. Road, Kolkata 700 009, INDIA

[2]Department of Environmental, Earth & Atmospheric Sciences

Intercampus Graduate School of Marine Sciences and Technology

University of Massachusetts Lowell

265 Riverside Street, Lowell, MA 01854-5045, USA

*Email: pngphy@caluniv.ac.in

#Email: robert_gamache@uml.edu

Abstract: Nitrogen-broadened water vapor line parameters of the (211)←(000) overtone band transitions in the 818-834 nm wavelength region are measured by using a tunable diode laser spectrometer. Water vapor is kept at its saturated vapor pressure at room temperature within a sample cell. Use of a balanced detector and a lock-in amplifier helps to increase the detection efficiency and the signal-to-noise ratio. The collisional broadening coefficients are extracted from the fitting of the experimental data by using a standard Voigt line profile. Collisional half-widths of water vapor lines perturbed by nitrogen are evaluated using the complex-valued implementation of the Robert-Bonamy (CRB) formalism. The wave functions and the energy eigenvalues in the (211) overtone band of water molecule are assumed on the basis of symmetry properties. Hence the outcome of this work also tests the validity of the theoretical approximations. The experimental data are compared with the corresponding theoretical values and the possible causes of deviation between the two have also been discussed.

Key words: N_2-broadening of water vapor, half-width, line shape/

INTRODUCTION

The water molecule is a very important trace gas constituent of the Earth's atmosphere. Its presence in the interstellar clouds and different planets like Mars, Venus, Saturn etc. has made it extremely important in astrophysics. Line parameters of water vapor rovibronic transitions in the near infrared and microwave region are used extensively in atmospheric science, remote sensing, pollution control, differential absorption LIDAR (DIAL) technique. Close monitoring of the global atmosphere is becoming more and more essential in view of ever-growing pollution. Water is a species that plays a key role in "greenhouse" warming of Earth's atmosphere. Knowledge of the spectral characteristics of water is important to properly interpret the results of remote sensing measurements as it will help to know the cause of atmospheric change and its effects. The collisional broadening parameters of water vapor rovibronic transitions are also utilized in radiative sensing of combustion and propulsion processes, radiative transfer modeling, gas dynamics and aerodynamics. Ar-broadening of water vapor rovibronic transitions is useful in combustion-kinetics research. Broadening of molecular transitions by He, Ar, N_2, O_2 and air [1-9] provides information that is helpful in developing the theory of intermolecular interactions based on the Complex Robert-Bonamy (CRB) model [10]. The theoretical modeling often helps in better understanding of the physical process. Complex Robert-Bonamy theory were used extensively for calculating the line parameters like collisional half-widths and line shifts using different absorbers like ozone, water vapor etc. in the presence of perturbers like oxygen, nitrogen, air, argon etc [11-13].

FTIR and diode laser spectrometers are extensively used for [1-9] measuring the line parameters of gas samples like water vapor, ammonia etc. Earlier we used a tunable diode laser spectrometer to study the argon and air broadened water vapor transitions belonging to the same overtone band [4-7]. In this work we have used this tunable diode laser spectrometer to measure the line parameters of thirteen ro-vibronic transitions of the (211)←(000) overtone band of water vapor, perturbed by nitrogen, in the 818-834 nm wavelength region. The nitrogen broadening coefficients and line shifts of these transitions have also been evaluated using the Complex Robert-Bonamy formalism and theoretically determined nitrogen broadening coefficients are compared with the experimentally determined values.

EXPERIMENTAL SETUP

The characteristics of the emitted radiation from diode lasers depend on the operating current and temperature. Hence stable operation of such a laser diode requires precision current and temperature controllers. The complete description of the current and temperature controllers, fabricated in the laboratory, has been published separately [7]. The Doppler widths of weak overtone transitions of specimens like acetylene, ammonia, water vapor etc. are of the order of 1 GHz at room temperature (296 K). In order to probe such transitions, a diode laser system should have a temperature stability of ~ 30 mK and current stability of a few μA. The current and temperature controllers of our diode laser system are stable up to ±10 μA and ±10 mK respectively, hence they are appropriate for studying the line parameters of weak overtone transitions of gas samples like water

vapor, acetylene etc. HL8311E and HL8314E GaAlAs laser diodes from Hitachi Ltd. have been used in this work. The typical tuning rates of HL8311E are ~3.3 GHz/mA and ~23.5 GHz/K and that of HL8314E are ~3.5 GHz/mA and ~24 GHz/K. We applied wavelength modulation technique to record the transitions. To implement this scheme, the diode laser drive current is modulated by 5 kHz, ±10 μA peak-to-peak sinusoidal signal. Very low modulation amplitude reduces the residual amplitude modulation (RAM) noise and at 5 kHz modulation frequency the *1/f* noise is also minimum.

Figure 1 shows the experimental arrangement. The laser diode is placed in a laser mount. A quarter-wave plate is placed in front of the laser to prevent direct optical feedback of the laser beam from optical components to the laser cavity. The output beam of the laser diode is divided into four parts out of which two are passed through a sample glass cell and an identical reference glass cell respectively. The glass cells are 1.5m in length and are fitted with optical windows. The beams coming out of the two cells are focused on two identical UDT 455 Si photodiodes of a balanced detector. The reference signal is subtracted from the sample signal by an OP177 precision operational amplifier (CMRR 130 db, offset voltage ~ 10μV and drift ~ 0.1μV/^{0}C) [4]. The output of the balanced detector is then fed to an Ithaco 3962A single phase lock-in amplifier to carry out phase sensitive detection at 5 kHz. The lock-in amplifier is set to provide the first derivative signal of the transitions. One of the remaining two parts of the laser beam is focused on the probe of a digital wavemeter (Wavemaster, Coherent; resolution = 0.01cm^{-1}) and the other part is passed trough a Fabry-Perot air-spaced etalon (FSR=5 GHz, finesse=36). The digital output of the wavemeter gives a direct readout of the emission frequency of the diode laser and hence it is very helpful in identification of the

water vapor transitions. The beam coming out of the etalon is detected by a single photodetector. The output of this photodetector is the input to a SR510 single phase lock-in amplifier. The etalon signal is used to determine the tuning rate of the diode lasers. The frequency axis of the recorded spectra is generated by using this tuning rate. The single mode emission regions of the diode lasers are identified with the help of the etalon and the wavemeter. To interface the data acquisition system with the computer, we have used a National Instrument GPIB 488.2 card.

Water vapor is kept at its saturated vapor pressure (20 Torr) at room temperature within the sample cell whereas the reference cell is maintained at a pressure of 10^{-2} Torr with the help of a rotary vane pump. Perturber gas (N_2) is introduced into the sample cell in steps of 40 Torr to carry out pressure dependent line shape measurements at different perturber pressures. A Baratron gauge (MKS, resolution=0.1 Torr) is used to measure the sample cell pressure. The water molecules are adsorbed by the wall of the sample glass cell at a rate of 2 Torr/hour (consistent with ref. [3]). The measurement time of each transition is only 1 minute; within this time period the change in pressure within the sample cell due to adsorption of water molecules by the glass cell wall would be around 0.03 Torr. Once the water vapor pressure in the sample cell reaches 20 Torr, the perturber gas is introduced within the cell and the measurement is carried out [4-7]. Hence the pressure within the sample cell remains almost unchanged during the measurement and small fluctuation of absorber pressure within the cell has very little effect on the line shape of the recorded transition. All the measurements are conducted at room temperature (296±1 K). The leak rate of the system is found to be less than 1 Torr/hour as measured with the help of a Pirani gauge.

Diode laser emission is often disturbed by the presence of mode breaks. The emission characteristic of each diode laser is first checked by thermally tuning the base plate temperature of its mount from 40^{o}C to 14^{o}C. Change in base plate temperature produces a change in both the temperature of the diode and its emission wavelength. This reveals the mode breaks and the wavelength range covered by the diode. The water vapor transitions falling within the emission wavelength range of a diode are also revealed by the thermal scan. Figure 2 shows the thermal scan of an HL8314E diode laser operating in the 833 nm wavelength region. We have set the integration time constant of the PI (proportional + integrator) control loop of the temperature controller to a high value (~ 3.5s) to ensure a slower response to the preset value of temperature [4-7], hence the transitions are clearly resolved during a thermal scan. The advantage of recording both the diode temperature and drive current during a thermal scan helps to adjust the temperature and current of the diode laser at the time of recording each individual water vapor transition by current scan. To record each individual transition, the diode drive current is scanned at a fixed temperature by applying a computer-controlled ramp signal. The high integration time constant of the PI control loop of the temperature controller stops short term cycling of temperature over the preset value during slow current ramp (ramp time = 30s). The lock-in time constant is kept fixed at 300 ms throughout the experiment.

LINE SHAPE SIMULATION

The transmitted intensity, I(ω), through a sample cell of length 'l' is related to the incident intensity, $I_o(\omega)$, by the Beer-Lambert's law:

$$I(\omega) = I_o(\omega) \exp[-\alpha(\omega)\, p\, l], \tag{1}$$

where p is the sample pressure and ω is the frequency of the radiation. The line shape function α(ω) is usually chosen as a standard Voigt profile which is the real part of a complex probability function and is expressed as follows:

$$\alpha_V(x,y) = A\left(\frac{y}{\pi}\right)\int_{-\infty}^{+\infty}\frac{\exp(-\tau^2)}{y^2+(x-\tau)^2}d\tau \tag{2}$$

Here, the subscript '*V*' to $\alpha(x,y)$ stands for the Voigt profile and τ is the dimensionless time parameter. The dimensionless parameters x and y are represented by $x = (\omega - \omega_o)/\sigma$ and $y = \gamma/\sigma$. σ is the Doppler half width at 1/e intensity of a spectral line and has a temperature dependence expressed as $\sigma = \omega_o(2kT/Mc^2)^{1/2}$ at a temperature T (in Kelvin). M is the molecular mass of the sample, k is the Boltzmann's constant and c is the speed of light. γ represents the collisional half width at half maximum (HWHM) of a spectral line due to phase perturbing collisions. 'A' stands for the line intensity and is related to the line strength parameter (S) through the equation $A = \sqrt{\pi}S/\sigma$. To simulate the theoretical line shape, we incorporated the line shape function shown by Eq. (2) in Eq. (1). There are three main contributions towards the error in the experimental profiles. These are — (a) pressure fluctuation inside the sample cell, (b) fluctuation in temperature in the surroundings and (c) slopping base line of the recorded signal. The error due to pressure and temperature fluctuations are quite small as discussed in the previous section.

We have used a balanced detector to minimize the base line noise and this also gives a flat base line [4-7]. The recorded *1f* spectra are numerically integrated, normalized and then fitted with the Voigt profile by using a non-linear least squares fitting program. In the fitting process, the line strength parameter (S) and the collisional half-width (γ) are kept as floating parameters whereas the Doppler width of the transition is kept fixed at its theoretical value at room temperature. The fitted collisional broadening parameters, Γ, (in cm^{-1}) are plotted against the perturber pressures (in Torr) for three different transitions at 12060.108, 12151.823 and 12195.190 cm^{-1} (Fig. 3). The error obtained from each fit of experimental line shape with the theoretical profile is shown in Fig. 3. The slope of the straight line obtained from a linear least squares fit gives the collision broadened half-width (γ) and the intercept on the ordinate gives the self broadening half-width of that transition. For each transition, the line strength parameter is determined for each pressure combination from the fit and the weighted average of all these values results in the final value of the line strength parameter [4-7]. These line strength parameters are given in Table 1 and compared to those of the same transitions reported in the HITRAN database [14] and our previous measurements [6].

THEORETICAL CALCULATIONS

The calculations are based on the complex implementation of the Robert-Bonamy (CRB) theory [10]. A description of the complex formalism has been given before [11-13], here only the salient features are presented. The method is complex valued so that the half-width and line shift are obtained from a single calculation. The dynamics are

developed to second order in time giving curved trajectories based on the isotropic part of the intermolecular potential [10], which has important consequences in the description of close intermolecular collisions (small impact parameters).

Within the CRB formalism the half-width, γ, and line shift, δ, of a ro-vibrational transition $f \leftarrow i$ are given by minus the imaginary part and the real part, respectively, of the diagonal elements of the complex relaxation matrix. In computational form the half-width and line shift are usually expressed in terms of the Liouville scattering matrix [15, 16]

$$(\gamma - i\delta)_{f \leftarrow i} = \frac{n_2}{2\pi c} \left\langle v \times \left[1 - e^{-{}^{R}S_2(f,i,J_2,v,b)} e^{-i[S_1(f,i,J_2,v,b)+S_2(f,i,J_2,v,b)]} \right] \right\rangle_{v,b,J_2} \qquad (3)$$

where n_2 is the number density of perturbers and $\langle ... \rangle_{v,b,J_2}$ represents an average over all trajectories (impact parameter b and initial relative velocity v) and initial rotational state J_2 of the collision partner. S_1 (real) and $S_2 = {}^{R}S_2 + i{}^{I}S_2$ are the first and second order terms in the expansion of the scattering matrix; they depend on the ro-vibrational states involved and associated collision induced jumps from these levels, on the intermolecular potential and characteristics of the collision dynamics The exact forms of the S_2 and S_1 terms are given in Refs. [11-13].

The S_1 term, which makes a purely imaginary contribution, is isotropic in the absence of any vibrational dependence of the anisotropic intermolecular forces. It is called the vibrational dephasing term and arises only for transitions where there is a change in the vibrational state. The potential leading to S_1 is written in terms of the isotropic induction and London dispersion interactions.

The $S_2 = {}^{R}S_2 + i{}^{I}S_2$ term is complex valued and results from the anisotropic interactions. The potential employed in the calculations consists of the leading

electrostatic components for the H_2O-N_2 (the dipole and quadrupole moments of H_2O with the quadrupole moment of N_2) and atom-atom interactions [17]. The latter are defined as the sum of pair-wise Lennard-Jones 6-12 interactions [18] between atoms of the radiating and the perturbing molecules. The heteronuclear Lennard-Jones parameters for the atomic pairs can be constructed from homonuclear atom-atom parameters by the "combination rules" of Hirschfelder et al. [19] or Good and Hope [20]. This work uses the definition of Hirschfelder et al. The atom-atom distance, r_{ij} is expressed in terms of the center of mass separation, R, via the expansion in 1/R of Sack [21]. Here the formulation of Neshyba and Gamache [17] expanded to eighth order is used.

Finally, recall that the isotropic component of the atom-atom potential, which in general is comprised of terms of the form $1/R^6$, $1/R^8$, $1/R^{10}$, etc., is used to define the trajectory of the collisions within the semiclassical model of Robert and Bonamy [10]. It is convenient to fit this summation to an effective isotropic (or "hetero-molecular") Lennard-Jones 6-12 potential. This approximation has no significant impact on our calculations other than to simplify the trajectory calculations.[12]

For water vapor, the reduced matrix elements are evaluated using wavefunctions determined by diagonalizing the Watson Hamiltonian [22] in a symmetric top basis for the vibrational states involved in the transition. For the ground state the Watson constants of Matsushima et al. [23] were used. For the $2\nu_1+\nu_2+\nu_3$ band Watson constants were not available so the Watson constants derived by Flaud and Camy-Peyret [24] for the ν_3 band were used so that the wavefunctions would have proper symmetry properties. The rotational constant for N_2 is 2.0069 cm^{-1} and that for O_2 is 1.4377 cm^{-1} [25].

Many of the molecular parameters for the H_2O-N_2 system are well known and the present calculations use the best available values from the literature. The dipole moment ($\mu = 1.8549\times10^{-18}$ esu) is taken from Shostak and Muenter [26]. The quadrupole moments of water vapor ($Q_{xx} = -0.13 * 10^{-26}$ esu, $Q_{yy} = -2.5 * 10^{-26}$ esu, $Q_{zz} = 2.63 * 10^{-26}$ esu) are taken from Flygare and Benson [27]. The quadrupole moment of nitrogen ($Q_{zz} = -1.4 * 10^{-26}$ esu) is from Mulder et al. [28]. The ionization potential of water is taken to be a vibrationally-independent value of 12.6 eV [29]. For nitrogen the polarizability, $17.4 * 10^{-25}$ cm^3, is taken from Ref. [30] and the ionization potential, 15.576 eV, from Ref. [31]. In the parabolic approximation, the isotropic part of the interaction potential is taken into account in determining the distance, effective velocity, and force at closest approach [10]. To simplify the trajectory calculations, the isotropic part of the atom-atom expansion is fit to an isotropic Lennard-Jones 6-12 potential.

In the present calculations, the line shape parameters have been calculated by explicitly performing the averaging over the Boltzmann distribution of velocities. The calculations also evaluate the mean relative thermal velocity (mrtv) approximation to the half-width. It has been shown [32] that at ~ 300K the mrtv calculation and the velocity averaged calculation give results within a few percent of one another, however the difference between the two methods of calculation is dependent on temperature [33].

The calculations were made for 13 transitions in the $2\nu_1+\nu_2+\nu_3$ band of H_2O broadened by N_2. The half-width and line shift were determined theoretically at the temperatures 200., 250., 296., 350., 500., 742., 980. K but the measurements were conducted at room temperature (296 K) only. Here the theoretical values at 296 K are reported to compare with the measurements. A clarification is necessary. Since the line

shape parameters, especially the line shift, depend on the vibrational state it is necessary to evaluate the S_1 term for the correct vibrational state, here the (211) and (000) vibrational states. However, as described above, wavefunctions for the upper state used the Watson constants of ν_3 band. This change affects the S_2 term for the upper state but the difference is generally small. The results of the calculations are presented in Table 1.

DISCUSSION & CONCLUSION

Table 1 shows both the measured and theoretically evaluated line parameters of thirteen water vapor ro-vibronic transitions perturbed by nitrogen. The reason for higher N_2-broadening coefficients compared to hydrogen, helium and argon broadening coefficients [3, 5, 6] may be explained from the high quadruple moment of N_2 molecule. The reason for lower broadening coefficients for Ar and He is that both Ar and He are nobel gas atoms, which interact with H_2O via the atom-atom potential hence the interaction is weaker. The measurement of oxygen broadening coefficients of these transitions is currently in progress and will be reported later. The studied transitions are mostly well isolated. Hence a single line fitting program has been used to extract the line parameters from the recorded spectra. But the transitions at 12013.665 and 12013.667 cm^{-1} are overlapping each other. So is the condition for the transitions at 12062.409 and 12062.500 cm^{-1}. We used a multi-line fitting program to fit the experimental profile with the theoretical Voigt line shape function for these overlapping transitions. The utilization of the multi-line fitting program to fit the overlapping transitions has been discussed earlier [6]. Figure 4 shows the measured values with the measured uncertainty compared

with the CRB calculated value plotted versus J"+0.8*Ka"/J" (This choice of axis coordinate was so that data would not overlap in the plot). The overall agreement is ~2.6 % but as the figure shows there are a number of lines with differences which are larger than 10%. The maximum difference between measurement and calculation is -20%. The average absolute percent difference between measurement and the CRB calculations is nearly 9%. The differences between measurement and theory do not appear to be related to the rotational quantum numbers, although there may not be enough transitions studied to observe the trends clearly. Part of the error may come from using approximate wave functions and energies in the calculations. However we estimate this to be less than 2 percent. This is under investigation. Another factor that may add a few percent errors is the choice of the intermolecular potential parameters. The atom-atom coefficients have been adjusted using the combination rules of Hirschfelder et al. [19] There are a number of different methods which have been proposed to determine heteronuclear potential parameters from homonuclear parameters [[34] and references therein, [35]]. Good and Hope [20] showed that different combination rules for ε lead to variations in ε of ~15%. The coefficients describing the vibrational dependence of the polarizability, which comes from an ab initio calculation [36], may also be questioned. It would be useful to adjust the intermolecular potential for H_2O-N_2 for use in the line shape calculations.

This is the first extensive study of the line parameters of the reported weak water vapor ro-vibronic transitions perturbed by nitrogen in the (211)←(000) overtone band in the 818-834 nm wavelength region using a tunable diode laser spectrometer. The line strength parameters of these transitions in presence of air and argon perturbers have been reported earlier [5-7, 37] and are consistent with the HITRAN database [14] and the work

from the Brussels-Reims groups [38, 39]. Earlier, Lucchesini et. al. [3] measured the line parameters of some water vapor overtone transitions belonging to the (211) band in this wavelength region using air as the perturber and the nitrogen broadening coefficient of only one transition (12053.370 cm^{-1}) was determined but detailed study of nitrogen broadening of these transitions had not been carried out. In our work, complex implementation of the Robert-Bonamy theory has been used to deduce the collisional half widths and line shifts of the experimentally studied transitions and the theoretical values are compared with the experimental results. In the next phase of work, we shall continue the measurement of line parameters of these water vapor overtone transitions with oxygen and carbon dioxide as the perturbers. Simultaneously, the line parameters will be determined theoretically. Use of polar and non-polar perturbers in measuring the half widths will ultimately enable us in further developing the theory of molecular interaction. We hope this study will be helpful in developing the database of water vapor overtone transitions.

Acknowledgements: A. B. thanks the Council of Scientific and Industrial Research, New Delhi for a research fellowship. B. R. and P. N. G. thank the FIST programme of the Department of Science and Technology, New Delhi for a research grant. Several authors (DLN and RRG) are pleased to acknowledge support of this research by the National Science Foundation (NSF) through Grant No. ATM-0242537. Any opinions, findings, and conclusions or recommendations expressed in this material are those of the author(s) and do not necessarily reflect the views of the National Science Foundation.

References:

(1) B. E. Grossmann, E. V. Browell, *J. Mol. Spectrosc.* **138,** 562-595 (1989).
(2) P. L. Ponsardin, E. V. Browell, *J. Mol. Spectrosc.* **185,** 58-70 (1997).
(3) A. Lucchesini, S. Gozini, C. Gabbanini, *Euro. Phys. J. D* **8,** 223-226 (2000).
(4) A. Ray, A. Bandyopadhyay, B. Ray, D. Biswas, P. N. Ghosh, *Appl. Phys. B* **79,** 915-921 (2004).
(5) A. Bandyopadhyay, A. Ray, B. Ray, P. N. Ghosh, *Chem. Phys. Lett.* **401,** 135-139 (2005).
(6) A. Bandyopadhyay, A. Ray, B. Ray, P. N. Ghosh, *J. Mol. Spectrosc.* **234,** 93-98 (2005).
(7) A. Ray, A. Bandyopadhyay, S. De, B. Ray, P. N. Ghosh, *J. Opt. Laser Tech.,* in press, (2006).

(8) V. Nagali, D. F. Davidson, R. K. Hanson, *J. Quant. Spectrosc. Radiat. Transfer* **64,** 651-655 (2000).
(9) A. Bruno, G. Pesce, G. Rusciano, A. Sasso, *J. Mol. Spectrosc.* **215,** 244-250 (2002).
(10) D. Robert, J. Bonamy, *J. Phys. Paris* **40,** 923-943 (1979).
(11) R. R. Gamache, R. Lynch, S. P. Neshyba, *J. Quant. Spectrosc. Radiat. Transfer* **59,** 319-335 (1998).
(12) R. Lynch, R. R. Gamache, S. P. Neshyba, *J. Quant. Spectrosc. Radiat. Transfer* **59,** 595-613 (1998).
(13) R. Lynch. Ph.D. dissertation. Department of Physics, University of Massachusetts Lowell 1995.
(14) L. S. Rothman, C. P. Rinsland, A. Goldman, S. T. Massie, D. P. Edwards, J.-M. Flaud, A. Perrin, C. Camy-Peyret, V.Dana, J.-Y. Mandin, J. Schroeder, A. Mccann, R. R. Gamache, R. B. Wattson, K. Yoshino, K. V. Chance, K. W. Jucks, L. R. Brown, V. Nemtchinov, P. Varanasi, *J. Quant. Spectrosc. Radiat. Transfer* **60,** 665-710 (1998).
(15) M. Baranger, *Phys Rev* **112,** 855-865 (1958).
(16) A. Ben-Reuven, Adv. Chem. Phys., S. A. Rice, Editor. Academic Press. p. 235 1975.
(17) S. P.Neshyba, R. R. Gamache, *J. Quant. Spectrosc. and Radiat. Transfer* **50,** 443-453 (1993).
(18) J. E. Jones, *Proc. R. Soc. A* **106,** 463-477 (1924).
(19) J. O. Hirschfelder, C. F. Curtiss, R. B. Bird, Molecular Theory of Gases and Liquids,. Wiley, (1964).
(20) R. J. Good, C. J. Hope, *J. Chem. Phys.* **55,** 111-116 (1971).
(21) R. A. Sack, *J. Math. Phys.* **5,** 260-268 (1964).
(22) J. K. G. Watson, *J. Chem. Phys.* **46,** 1935-1949 (1967).
(23) F. Matsushima, H. Odashima, T. Iwaskai, S. Tsunekawa, *J. Mol. Struct.* **352-353,** 371-378 (1995).

(24) J.-M. Flaud, C. Camy-Peyret. Watson Hamiltonian constants for low lying vibrational states of H_2O, Private Communication, 2005.
(25) K. P. Huber, G. Herzberg, Molecular Spectra and Molecular Structure: Constants of Diatomic Molecules. New York: Van Nostrand, (1979).
(26) S. L. Shostak, J. S. Muenter, *J. Chem. Phys.* **94,** 5883-5890 (1991).
(27) W. H. Flygare, R. C. Benson, *Mol. Phys.* **20,** 225-250 (1971).
(28) F. Mulder, G. V. Dijk, A. Van der Avoird, *Mol. Phys.* **39,** 407-425 (1980).
(29) D. R. Lide, ed. CRC Handbook of Physics and Chemistry. 83rd ed, The Chemical Rubber Company, Clevland, OH, 2003.
(30) M. P. Bogaard, B. J. Orr, Chapter 5, MPT International Review of Science, Physical Chemistry, Series Two, Vol. 2. Molecular Structure and Properties, A. D. Buckingham, Editor. Butterworths: London 1975.
(31) A. Lofthus, The molecular spectrum of nitrogen. 1960, Department of Physics, University of Oslo, Blindern, Norway.
(32) R. R. Gamache, L. Rosenmann, *J. Mol. Spectrosc.* 488-499 (1994).
(33) R. R. Gamache, *J. Mol. Spectrosc.* **208,** 79-86 (2001).
(34) M. Diaz Pena, C. Pando, J. Renuncio, A. R., *J. Chem. Phys.* **76,** 325-332 (1982).
(35) M. Diaz Pena, C. Pando, J. A. R. Renuncio, *J. Chem. Phys.* **76,** 333-339 (1982).
(36) Y. Luo, H. Agren, O. Vahtras, P. Jorgensen, V. Spirko, H. Hettema, *J. Chem. Phys.* **98,** (1993).
(37) A. Bandyopadhyay, A. Ray, B. Ray, P. N. Ghosh, Proceedings, International Conference on Optics & Optoelectronics, Dehradun, India, OP-LA 11, 2006
(38) M. F. Merienne, A. Jenouvrier, C. Hermans, A. C. Vandaele, M. Carleer, C. Clerbaux, P. F. Coheur, R. Colin, S. Fally, M. Bach, *J. Quant. Spectrosc. Radiat. Transfer* **82,** 99-117 (2003).
(39) S. Fally, P. F. Coheur, M. Carleer, C. Clarbaux, R. Colin, A. Jenouvrier, M. F. Merienne, C. Hermans, A. C. Vandael, *J. Quant. Spectros. Radiat. Transfer* **82,** 119-131 (2003).

Table 1. Collision broadening coefficients (γ) and line shifts (δ) in cm^{-1}/atm for water vapor transitions broadened by nitrogen at 296 K. The terms within the parenthesis in the columns of 'γ^*(Observed)' and the column of 'line strength' represent the errors obtained in the fitting process. The fitted values of the line strength parameters are compared with those given in the HITRAN database (38) and ref. 6.

Transition (cm^{-1})	(211)←(000)						Line strength ($\times 10^{23}$) (cm/molecule)			H_2O-N_2			
	J'	K_a'	K_c'	J	K_a	K_c	HITRAN	Ref.6	Present work	γ^* (Observed)	γ (CRB)	%Difference	δ
11988.494	6	0	6	7	0	7	1.011	0.962(6)	0.984(9)	0.0811(20)	0.0757	6.68	-0.0201
11988.725	6	1	6	7	1	7	0.335	—	0.331(10)	0.0772(30)	0.0746	3.40	-0.0199
12001.968	5	2	4	6	2	5	0.829	0.667(6)	0.811(8)	0.1057(43)	0.0878	16.98	-0.0125
12013.665	4	2	2	5	2	3	1.239	1.104(7)	1.261(8)	0.1002(26)	0.0893	10.89	-0.0157
12013.667	5	0	5	6	0	6	0.554	0.519(8)	0.581(9)	0.1126(24)	0.1041	7.54	-0.0072
12014.146	5	1	5	6	1	6	1.663	1.504(6)	1.719(9)	0.0963(26)	0.0872	9.40	-0.0158
12060.107	3	0	3	4	0	4	1.040	0.985(6)	1.064(8)	0.0988(29)	0.1078	-9.07	-0.0102
12062.409	3	1	3	4	1	4	3.022	2.883(5)	3.056(6)	0.1206(27)	0.1050	12.92	-0.0099
12060.500	4	0	4	4	2	3	0.180	0.159(7)	0.192(18)	0.1079(13)	0.1042	3.42	-0.0128
12151.823	2	2	0	2	2	1	3.902	—	3.974(6)	0.1096(9)	0.1037	5.36	-0.0075
12153.702	3	2	1	3	2	2	0.590	—	0.624(7)	0.0946(26)	0.1041	-10.06	-0.0073

12156.208	1	1	0	1	1	1	0.982	—	1.032(8)	0.1097(23)	0.1139	-3.79	-0.0036
12195.190	2	0	2	1	0	1	3.544	—	3.743(8)	0.0958(10)	0.1150	-20.00	-0.0040

Figure captions:

Figure 1. Block diagram of the experimental set-up. CC: current controller. TC: temperature controller. LDM: laser diode mount. QWP: quarter wave plate. BS: beam splitter. E: etalon. D1, D2, D3: photodetectors. SC: sample cell. RC: reference cell. PG: Pirani gauge. B: Baratron. PC: personal computer. DAQ: data acquisition system. LO: local oscillator. LIA: lock-in amplifier. BD: balanced detector. W: wavemeter. Mod: modulation.

Figure 2: Thermal scan of the laser diode HL8314E (833.6nm) from 40^{o}C to 24^{o}C. (A) First derivative spectrum of water vapor transitions; (B) etalon signal. The transition at 11988.494 cm^{-1} is recorded at a signal to noise (S/N) ratio of 60 and the transition at 12027.751 cm^{-1} is recorded at an S/N ratio of 13.

Figure 3 Plot of collisional broadening coefficient (cm^{-1}) vs. perturber pressure (Torr) for the water vapor transitions at (A) 12151.823 cm^{-1}, (B) 12060.108 cm^{-1} and (C) 12195.190 cm^{-1}. The straight lines are the linear fits of the data points and the vertical bars at each data point give the error obtained in the fitting process. Water vapor pressure inside the sample cell is 20 Torr at 296 K.

Figure 4 Plot of measured nitrogen broadened half-widths with the measured uncertainties and the calculated nitrogen broadened half-widths using CRB formalism versus J”+ 0.8*Ka”/J”.

Figure 1

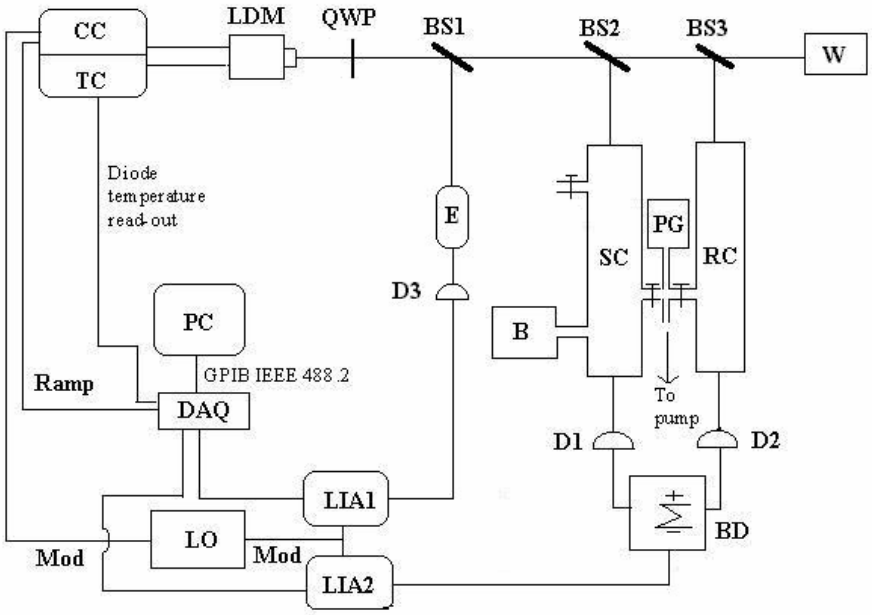

Fig.1

Figure 2

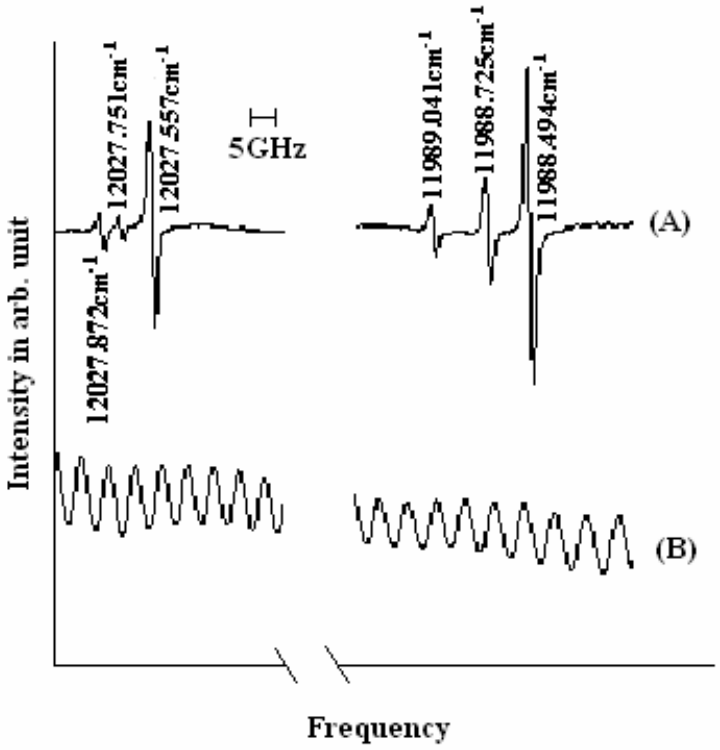

Fig:2

Figure 3

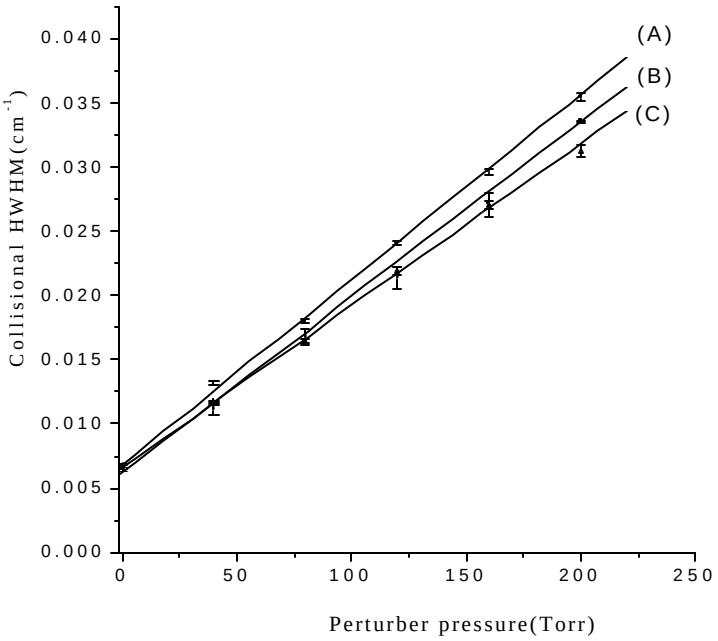

Fig: 3

Figure 4